Supplemental Material

Supporting Information for

Why do precipitation intensities tend to follow Gamma distributions?

Cristian Martinez-Villalobos and J. David Neelin

October 22, 2019

Section S1: Effect of neglecting $E + \bar{C}$ in the wet regime

The solution in the case where $E + \bar{C}$ is not neglected in the wet regime has the same shape as the solution with $E + \bar{C}$ neglected (eq. 9 in main text), but with parameters (denoted with a *) given by

$$\bar{s^*} = \frac{\bar{s}}{(1-\delta)} \approx \bar{s}(1+\delta), \qquad s_L^* = \frac{s_L}{(1-\delta)^2} \approx s_L(1+2\delta), \tag{1}$$

with $\delta = \frac{E+\bar{C}}{R_0} << 1$. That is, the main effect of including $E + \bar{C}$ in the solution is is a slight extension of the cutoff scale. This can be seen in Fig. S2a, which compares the analytical solutions for the $E + \bar{C}$ neglected and non-neglected cases. Figure S2b confirms numerically the analytical results for the on-off case, and Fig. S2c shows numerically that the main modification to the solution carries over to the ramp precipitation case.

Section S2: Event duration distribution and $s_L \propto \sqrt{t_L} D_P$ in the ramp precipitation model

The solution for the wet spell duration probability distribution in the ramp precipitation case, adapted from Yi (2010), is given by

$$p_t = \frac{b}{\sqrt{2\pi D_P^2}} exp\left(-\frac{b^2 \alpha exp(-\alpha t)}{2D_P^2 sinh(\alpha t)} + \frac{\alpha t}{2}\right)\left(\frac{\alpha}{sinh(\alpha t)}\right)^{3/2}. \tag{2}$$

To an excellent approximation we can simplify this to

$$p_t = \frac{\bar{t}}{\sqrt{\pi t_L}} exp(-\frac{\bar{t}^2}{t_L t})[2^{-1} t_L (1 - exp(-\frac{2\bar{t}}{t_L}))]^{-3/2} exp(-\frac{t}{t_L}), \tag{3}$$

where t_L is the duration cutoff given by

$$t_L = \frac{1}{\alpha}, \tag{4}$$

and where we have also defined $\bar{t} = \frac{b}{\sqrt{2\alpha D^2}}$. After making these definitions, expressions for p_t in the on-off (eq. B1 in main text) and ramp precipitation models are similar, with the expression $[2^{-1} t_L (1 - exp(-\frac{2\bar{t}}{t_L}))]^{-3/2}$ providing an approximate power law range in the ramp case.

The proportionality $s_L \propto \sqrt{t_L} D_P$, that was derived analytically in the on-off model (eq. 11 in main text), is shown numerically to hold in the ramp precipitation case. Figure S3a shows that the accumulation moment ratio s_M (which is proportional to s_L, see Section S4) is linearly proportional to $\sqrt{t_L}$, with t_L given by eq. 4 in the SI, when we keep D_P fixed. Similarly, Fig. S3b shows that s_M is linearly proportional to D_P when we keep t_L fixed.

Section S3: Derivation of accumulation distribution mathematical form in the on-off precipitation model.

The derivation of the accumulation distribution (eq. 9 in main text) in the on-off case is shown in SN14 and N17 —here we present its main steps for the reader's convenience. Noting that in the on-off precipitation case the accumulation in an event is proportional to its duration ($s = R_0 t$), the column water vapor equation in the wet regime (eq. 6 in main text) can be written in a transformed s coordinate (see N17 for more details) as

$$\frac{dq}{ds} = -1 + D_s \eta_s, \tag{5}$$

where $D_s = \frac{D_P}{R_0^{1/2}}$ and η_s is white noise in s coordinate. The Fokker-Planck equation (Gardiner 2009) governing the evolution (in s coordinate) of the probability of column water vapor in the wet regime $p_q(s,q)$ is given by

$$\frac{\partial p_q}{\partial s} = \frac{\partial p_q}{\partial q} + \frac{1}{2} D_s^2 \frac{\partial^2 p_q}{\partial q^2} = -\frac{\partial J}{\partial q}, \tag{6}$$

where $J = -p_q - \frac{1}{2} D_s^2 \frac{\partial p_q}{\partial q}$ is the probability flux (such that $\frac{\partial p_q}{\partial t} + \frac{\partial J}{\partial q} = 0$). The solution $p_q(s,q)$, subjected to the initial condition $p_q(s = 0, q) = \delta(q - q_c)$ and absorbing boundary condition $p_q(s, q = q_{np}) = 0$ (with $q_c = q_{np} + b$, as defined in section 3a in the main text) is given by the pair of Gaussians

$$p_q(q,s) = \frac{1}{\sqrt{2\pi D_s^2 s}} \left[exp\left(-\frac{(q - q_c + s)^2}{2 D_s^2 s} \right) - exp\left(\frac{2b}{D_s^2} \right) exp\left(-\frac{(q - q_c + 2b + s)^2}{2 D_s^2 s} \right) \right]. \tag{7}$$

The accumulation distribution is given by the probability flux evaluated at event termination. Noting that $p_q|_{q=q_{np}} = 0$, then

$$p_s = J|_{q=q_{np}} = -\frac{1}{2} D_s^2 \frac{\partial p_q}{\partial q}\bigg|_{q=q_{np}}, \tag{8}$$

which after evaluating yield the analytical solution for p_s shown in eq. 9 in the main text.

In a simpler system with no moisture loss by accumulation (no -1 term in eq. 5 in the SI), the solution for p_q is much like eq. 7 but without the s term in the numerator of the exponentials. In this case, it can be readily seen from eq. 8 that p_s would have a power law range with exponent $\tau = 1.5$, as the derivative brings an additional s^{-1} term to the expression for p_s. In the more general case (with moisture loss by accumulation) p_s inherits the power law range from the simpler system, but with the added exponential $exp(-s/s_L)$ that limits the very large accumulation values.

Section S4: Relation between accumulation moment ratio and cutoff

Assuming a shape of the accumulation distribution p_s given by (4) in the main text

$$P_s = B(s) s^{-\tau} exp(-\frac{s}{s_L}), \tag{9}$$

where $B(s)$ is a function that decay fast when $s \to 0$ (which is necessary to ensure proper normalization for $\tau > 1$). If we assume that $\tau < 2$, then we have that the small accumulation range does not overly contribute to the n-th accumulation moment $\langle s^n \rangle$. In this case we have that $\langle s^n \rangle$ is approximately proportional to $\int_0^\infty s^{-\tau+n} exp(-\frac{s}{s_L}) ds$. Expressing this in terms of Gamma functions Γ, we have that $\langle s^n \rangle \approx B_0 s_L^{n+1-\tau} \Gamma(n + 1 - \tau)$, where B_0 is some constant of proportionality. The moment ratio $s_M = \frac{\langle s^2 \rangle}{\langle s \rangle}$ is then given by

$$s_M \approx (2 - \tau) s_L, \tag{10}$$

where we have used the property $z\Gamma(z) = \Gamma(z + 1)$ of Gamma functions. This shows that s_M is approximately proportional to the cutoff, with constant of proportionality depending on τ ($s_L \approx$

$2s_M$ in the on-off case, where $\tau = 1.5$). So for example in Fig. 6 of main text, where the model parameters in the wet regime were chosen to yield similar s_M as in observations, the modeled and observed cutoffs may not be as similar, due to the different τ simulated compared to observations in Fig. 6b.

Figure S1: Correlation between P_L and τ_P estimators.

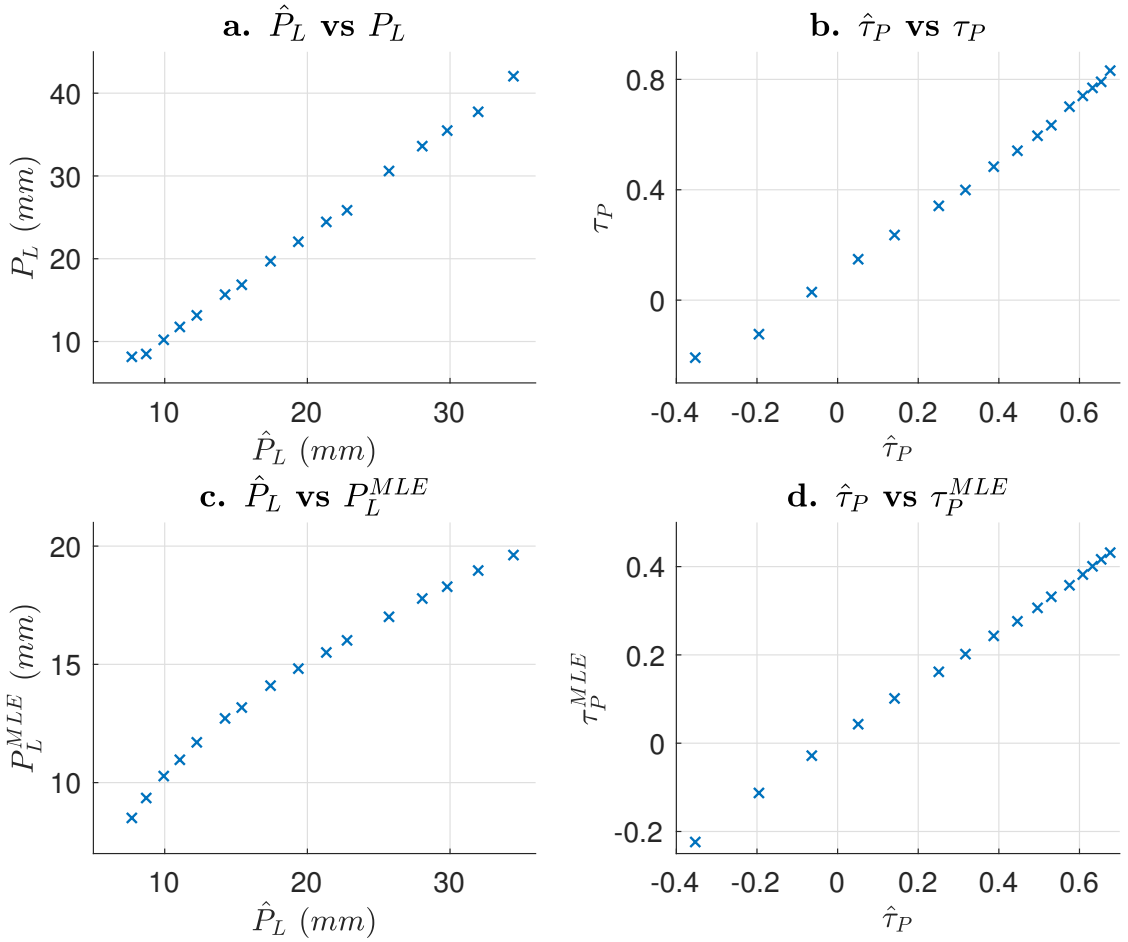

Figure S1: Scatter of estimators of **a)** daily precipitation cutoff, and **b)** power law exponent using the method of moments ($\hat{}$) and the regression technique shown in Appendix A of the main text (unadorned). **c),d)** Similar to **a),b)**, but comparing the method of moments with maximum likelihood (^{MLE}) following the method of Thom 1958. Estimations are calculated from 16 different 500 year integrations of the on-off precipitation model, with parameters $E = 0.1\frac{mm}{h}$, $\bar{C} = 0$, $D_E = 3\frac{mm}{h^{1/2}}$, $b = 1mm$, $P = 10\frac{mm}{h}$, and D_P varying from 5 to $20\frac{mm}{h^{1/2}}$ in increments of $1\frac{mm}{h^{1/2}}$. Correlation coefficients r between estimators are **a** 0.9994, **b** 0.9996, **c** 0.9895, **d** 0.9994.

Figure S2: Effects of neglecting $E + \bar{C}$ in the wet regime.

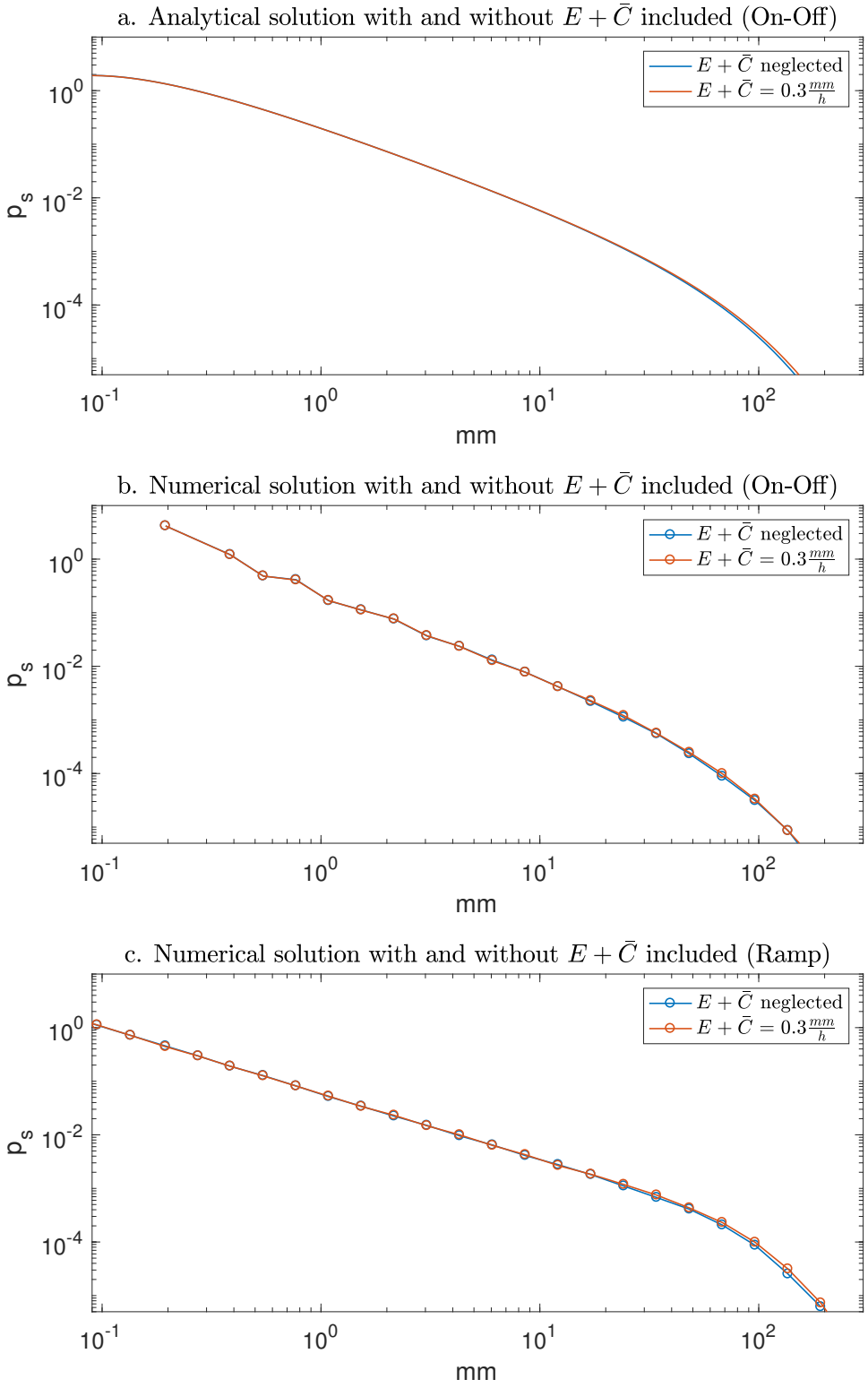

Figure S2: **a.** Analytical solution for the accumulation distribution in the on-off case for the cases where $E + \bar{C}$ in the wet regime is neglected (blue) and the case it is not (red). Solutions are constructed using the following parameters: $D_P = 15\frac{mm}{h^{1/2}}$, $E + \bar{C} = 0.3\frac{mm}{h}$, $P = 10\frac{mm}{h}$, $b = 1mm$. **b.** Result of two 200yr numerical integrations of the on-off model with the same parameters as (a). **c.** Numerical comparison of two 200yr integrations of the ramp model, one with $E + \bar{C}$ neglected and one where it is not ($E + \bar{C} = 0.3\frac{mm}{h}$). Same parameters as in (a), except with $\alpha = 0.3\frac{1}{h}$.

Figure S3: $s_L \propto \sqrt{t_L} D_P$ in the ramp model

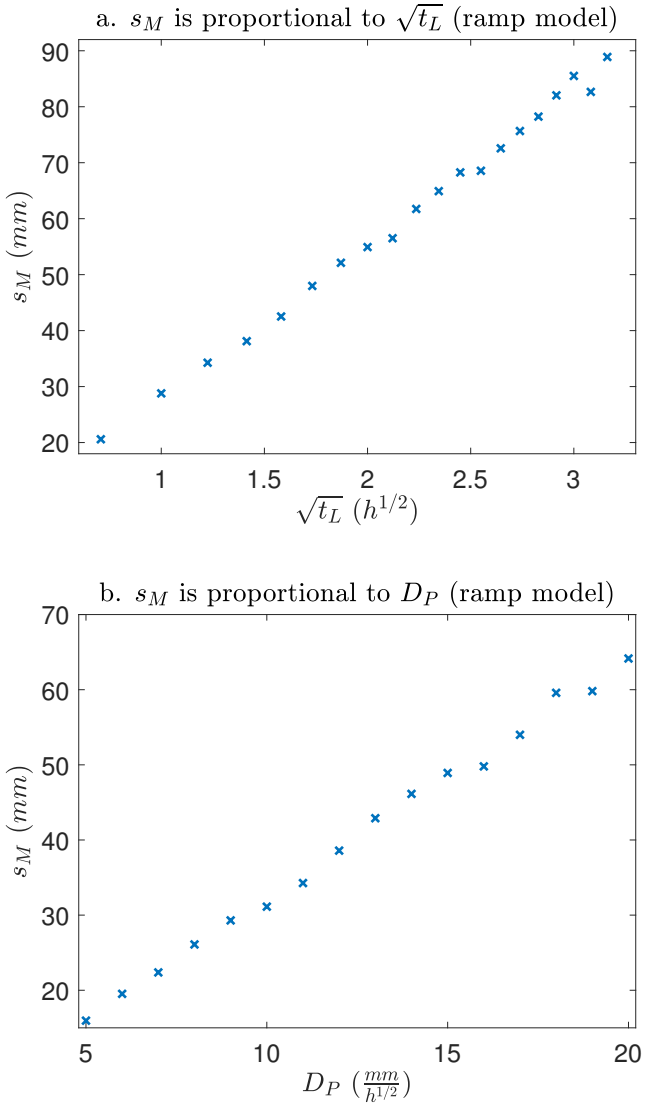

Figure S3: **a**. Scatter between s_M and $\sqrt{t_L}$ calculated for several 200yr runs of the ramp model with parameters $E = 0.1\frac{mm}{h}$, $\bar{C} = 0$, $D_P = 15\frac{mm}{h^{1/2}}$, $D_E = 3\frac{mm}{h^{1/2}}$, $b = 1mm$, and α varying such that the different runs have t_L values ranging from 30 minutes to 10 hours. **b**. Scatter between s_M and D_P calculated for several 200yr runs of the ramp model with same parameters as in (**b**), with D_P ranging from 5 to $20\frac{mm}{h^{1/2}}$ and $\alpha = \frac{1}{t_L} = \frac{1}{3}h^{-1}$.

Figure S4: Wet and dry regime effects on Gamma distribution parameters in the ramp precipitation model

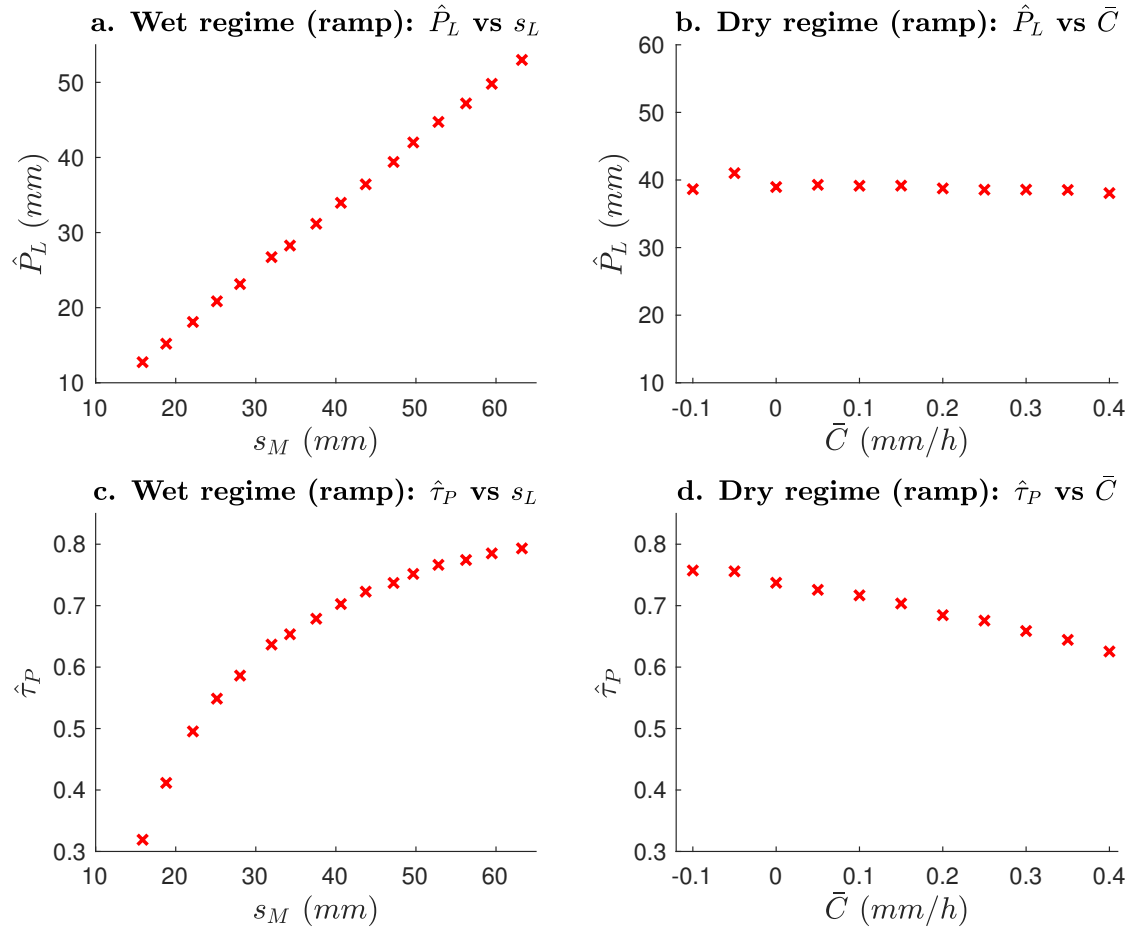

Figure S4: Same as Fig. 4 in main text but using the ramp precipitation model (with no analytical approximation in this case). Parameters are the same as Fig. 4 except $\alpha = 0.35h^{-1}$ replaces R_0. In this case there is no analytical formula for s_L so we use the accumulation moment ratio $s_M = \frac{\sigma_s^2 + \bar{s}^2}{\bar{s}}$ as its estimator, as used in previous publications (e.g., Peters et al., 2010, N17, MN18. See also Section S4).

Figure S5: $\frac{\sigma_w^2}{\bar{w}}$ as a function of changes in wet and dry regime dynamics

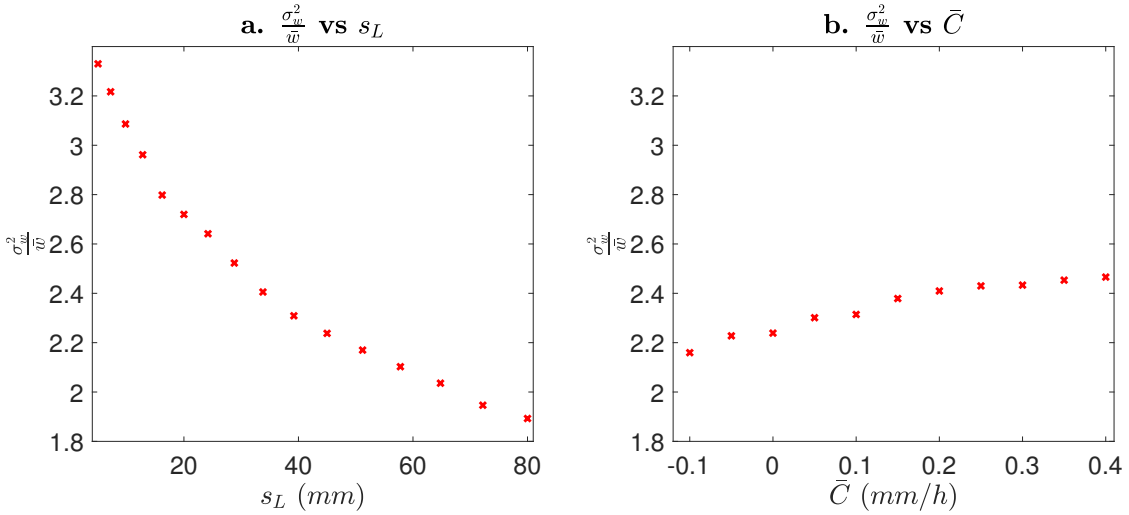

Figure S5: Ratio between variance and mean number of events per day $\frac{\sigma_w^2}{\bar{w}}$ as a function of changes in **a** s_L in the wet regime, and **b** $\bar{C}$ in the dry regime. This is calculated from the same 500yr model runs used in Fig. 4 in the main text. This shows that $\frac{\sigma_w^2}{\bar{w}}$ is of order 1 regardless of model parameters, which helps justify (19) in the main text.

Figure S6: Total number of events as a function of changes in wet and dry regimes dynamics

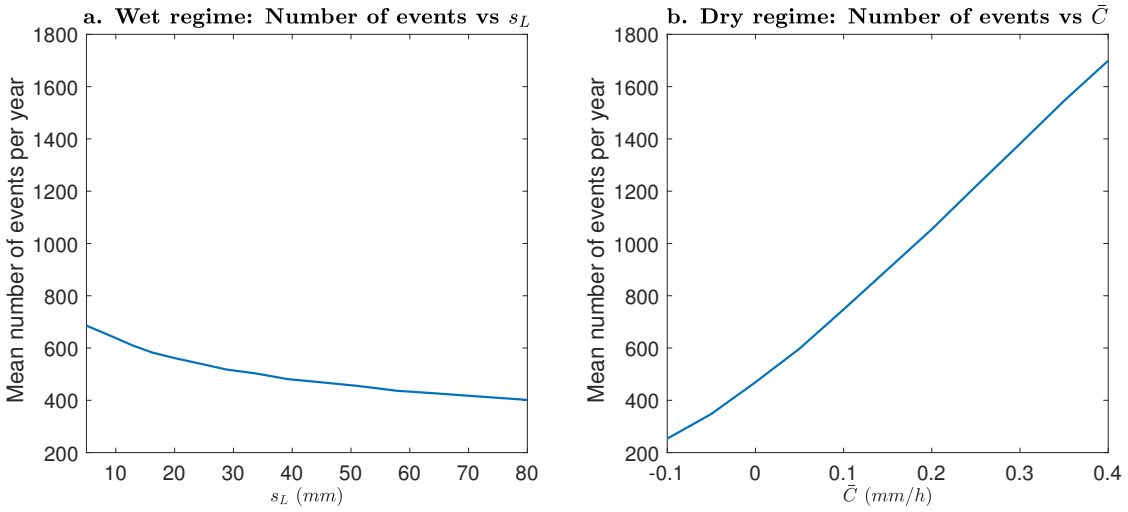

Figure S6: Number of accumulation events for different values of **a** s_L and dry regime parameters fixed, and **b** $\bar{C}$ and wet regime parameters fixed. This is calculated from the same model 500yr runs used in Fig. 4 in the main text.

Figure S7: Error in analytical approximation for $\hat{P}_L$ for different averaging intervals.

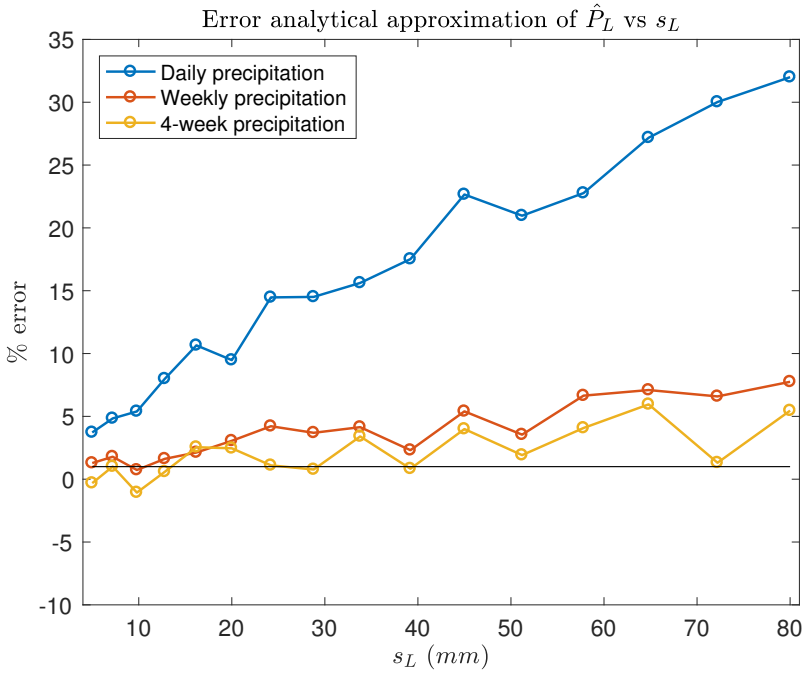

Figure S7: Error in the analytical approximation of $\hat{P}_L$ (equation 17 in main text) compared to $\hat{P}_L$ calculated directly from daily, weekly or 4-weeks data based on 500yr model runs for different D_P values, with same parameters as used in Fig. 4a in the main text. The error is calculated as the percentage deviation between the blue line and red crosses in Fig. 4a, and similarly for weekly and 4-weeks precipitation averages. The x-axis is the $s_L = \frac{2D_P^2}{R_0}$ corresponding to each individual run. This corresponds to a $t_L = \frac{2D_P^2}{R_0^2}$ ranging from 30 minutes ($s_L = 5mm$) to 8 hours ($s_L = 80mm$). This error is due to the assumptions made in section 4 that were used to derive the analytical expressions in section 5 of the main text.

Figure S8: Sensitivity to temporal resolution of data

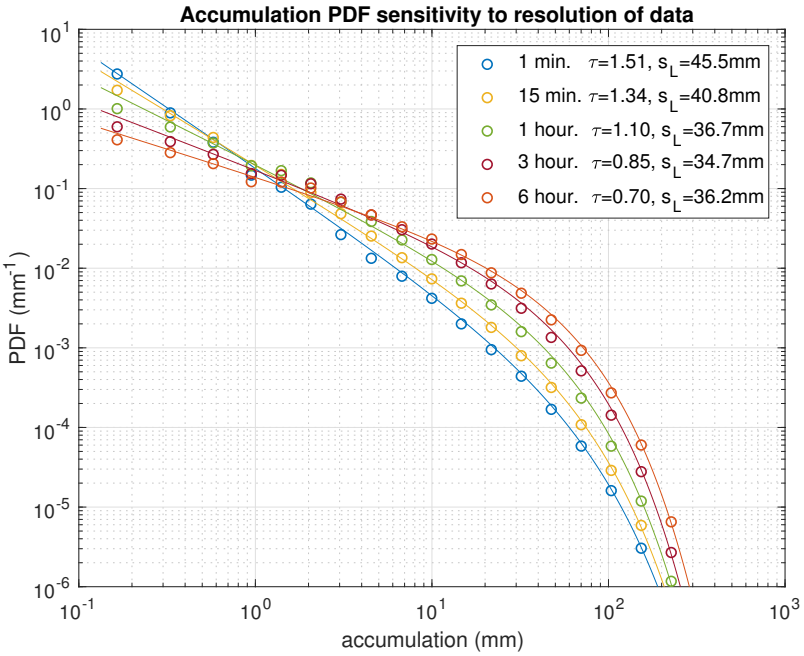

Figure S8: Sensitivity of accumulation distribution parameters τ and s_L to resolution of data. This is calculated from a 1000yr integration of the on-off precipitation model with a time step of one minute, with parameters $P = 10\frac{mm}{h}$, $E = 0.1\frac{mm}{h}$, $\bar{C} = 0$, $D_P = 15\frac{mm}{h^{1/2}}$, $D_E = 3\frac{mm}{h^{1/2}}$, $b = 0.2mm$, $q_c = 65mm$. In each of the cases shown here the 1-minute simulated data is accumulated into 15 minutes, 1 hour, 3 hours and 6 hours accumulated values, which are used as building blocks to calculate the accumulation distributions. Theoretical values for the parameters in this case are $s_L = 45mm$ and $\tau = 1.5$.

Figure S9: Accumulation and temporally averaged precipitation distributions in two other locations

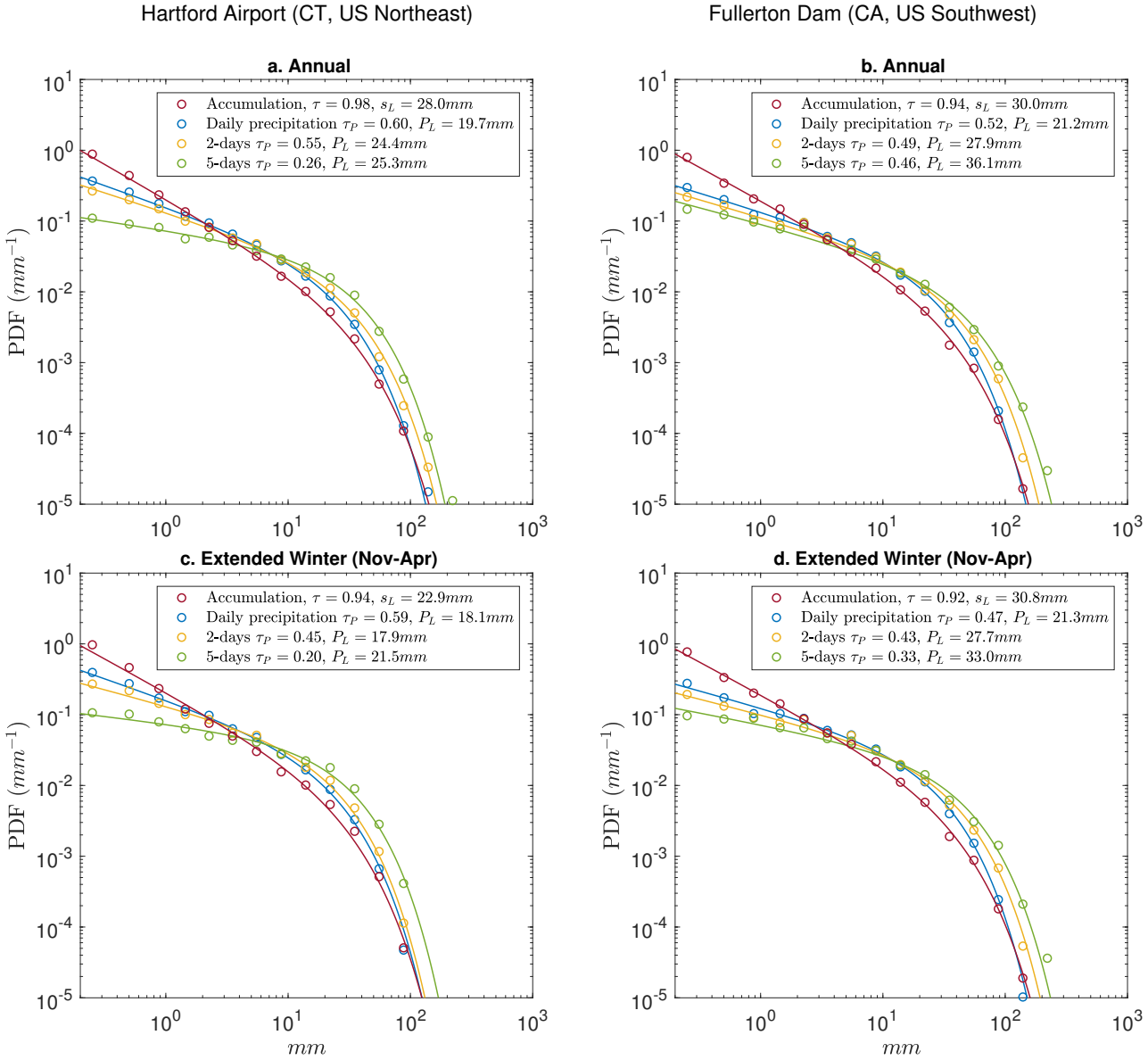

Figure S9: Similar to Fig. 6b in the main text but for other locations: **a.** Hartford Bradley International Airport (1954-2013, 64.9m altitude, $41^o56'N$, $287^o19'E$), **b.** Fullerton Dam (1948-2013, 103.6m altitude, $33^o54'N$, $242^o7'E$). **c.** Similar to **a** but only for the extended winter months (Nov-Apr). **d.** Similar to **b** but only for the extended winter months (Nov-Apr). The Hartford Airport area sees precipitation both in winter (predominantly snow) and summer (predominantly convective). Almost all precipitation in the Fullerton Dam area occurs in winter and has a predominantly frontal origin.

Figure S10: w_n becomes more localized around the mean as t_{avg} increases

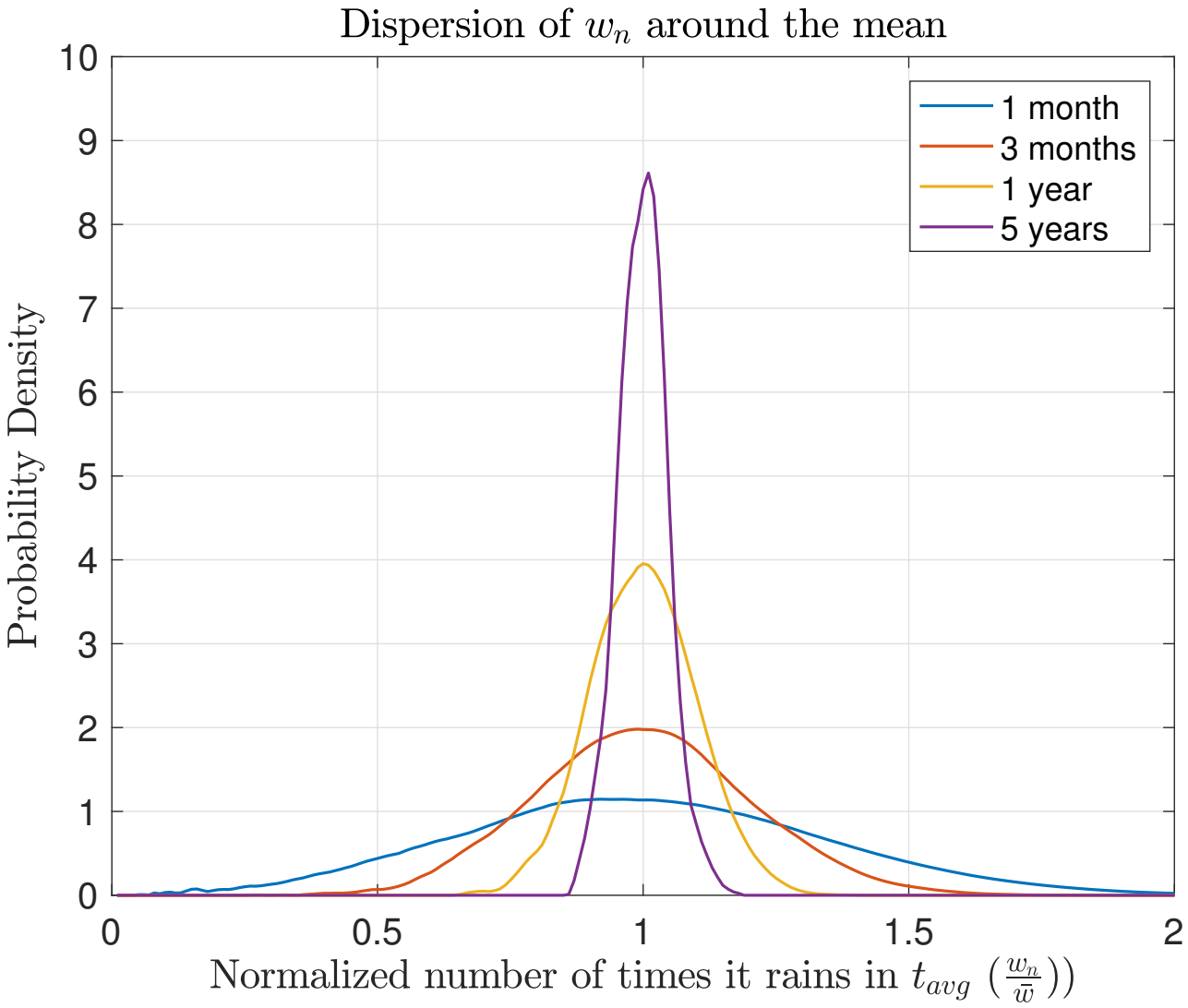

Figure S10: Normalized number of events distribution $\frac{w_n}{\bar{w}}$ for different t_{avg}. The size of the fluctuations relative to the mean $\frac{\sigma_w}{\bar{w}}$ decreases as $\bar{w}^{-1/2}$. Distributions are calculated from a 2000 years integration of eqs. 5,6,8 in the main text for mean moisture convergence conditions $\bar{C} = 0.2\frac{mm}{h}$, as this tightening of the distribution around $\bar{w}$ occurs faster under these conditions. Remaining parameters are $R_0 = 10\frac{mm}{h}$, $E = 0.1\frac{mm}{h}$, $D_P = 15\frac{mm}{h^{1/2}}$, $D_E = 3\frac{mm}{h^{1/2}}$, $b = 1mm$.

Table S1: Parameters used to generate main text figures

	R_0 $(\frac{mm}{h})$	α $(\frac{1}{h})$	D_P $(\frac{mm}{h^{1/2}})$	$\bar{C}$ $(\frac{mm}{h})$	b (mm)
Fig. 2b	9	N/A	17	0.2	0.2
Fig. 2c	N/A	0.35	12	0.2	0.2
Fig. 3	10	N/A	15	0	1
Fig. 4a,c	10	N/A	5 to 20	0	1
Fig. 4b,d	10	N/A	15	-0.1 to 0.4	1
Fig. 5a,c,e	10	N/A	10,15,20	0	1
Fig. 5b,d,f	10	N/A	15	-0.1, 0.1, 0.3	1
Fig. 6	9	N/A	17	0.2	0.2
Fig. 7	10	N/A	15	-0.1, 0.2	1
Fig. 8	N/A	0.3	15	0	1

Table S1 Parameters used in all main text figures. The following parameters are the same in all cases: $E = 0.1\frac{mm}{h}$, $D_E = 3\frac{mm}{h^{1/2}}$, and $q_c = 65mm$.